RESEARCH PAPER

Modeling of Temperature Dependency of Silicon Nitride Formation's Kinetics during Reaction Bonded Method

E. Shahmohamadi, A. Mirhabibi and F. Golestanifard

**ar.mirhabibi50@gmail.com*

Received: January 2019 **Revised: May 2019** **Accepted: June 2019**

School of Metallurgy and Materials Engineering, Iran University of Science and Technology, Tehran, Iran.

DOI: 10.22068/ijmse.16.2.52

Abstract: *An accurate prediction of reaction kinetics during silicon nitridation is of great importance in designing procedure of both material production and controlling of reaction. The key purpose of the current research is to study the consequence of temperature on the formation kinetics of reaction bonded silicon nitride (RBSN). To do so, nitrogen diffusion in the silicon nitride layer is deliberated as a reaction controlling factor and sharp interface technique based on this theory is used to improve the analytical model. In this developed model, the variations in the size of silicon particles are considered for the entire reaction. In the experimental phase, the extent of nitridation is measured for different reaction temperatures and 4 different reaction times and at that time, the incidence of full nitridation is shown by EDS analysis. Furthermore, an analytical approach was established for describing the kinetics of compound formation and the performance of the developed model evaluated through statistical analysis. There was good superposition among experimental data and calculations of the developed model which establishes the accuracy of considered presumptions and reaction mechanisms.*

Keywords: *Reaction bonded silicon nitride (RBSN), Kinetic Modeling, Silicon Nitride, Sharp interface model (SIM), Diffusion Control.*

1. INTRODUCTION

Silicon nitride (Si_3N_4) is one of the most used important high-temperature engineering ceramics due to its excellent properties such as good heat resistivity as a refractory, thermal shock resistance, chemical stability, creep and wear resistance even at high temperatures preserving its desirable characteristics to be used in related industrial applications [1-4]. During sudden thermal shock, due to the low coefficient of thermal expansion (CTE), the silicon nitride does not easily crack or even deform. This case introduces the mentioned compound as good refractory material and is used in high-temperature applications such as cutting tools, metal casting tools, bearings, glow plugs, turbocharged rotors, etc. [5]. Also due to its excellent mechanical performance and enhanced thermal conductivity with respect to other ceramics, Si_3N_4 is considered as a potential heat dissipation substrate in high-power electronic devices [6, 7]. To produce a nitride silicon body, various processing methods are used as hot press, hot isostatic press, pressureless sinter, gas partial pressure press, reaction bonded, sintered reaction bonded. The investigated method proposed in this study is a reaction-bonded silicon nitride which yields near-net-shape components compared to other methods due to slight shrinkage during the reaction and preserving its final dimensions. This method is performed in lower temperatures and the raw material is silicon powder which is quite cost-effective compared to silicon nitride powder.

This process is based on the heterogeneous gas-solid reaction of silicon powder in the nitrogen atmosphere. Silicon nitride can be formed by the reaction of silicon powder in the atmosphere of nitrogen (reaction 1).

$$3Si_{(s)} + 2N_{2(g)} \rightarrow Si_3N_{4(s)} \quad (1)$$

Because of requiring much more time to complete the nitridation reaction by reaction bonded compare to other methods and melting of unreactive silicon due to heat release from the reaction, controlling of reaction conditions to produce high-quality ceramics and preventing typical process problems (cracking or intumescing) is necessary. Thus, to control the reaction, know-

ing about the effect of kinetic factors on reaction rate is actually vital to design pieces in production or control line. When the chemical reaction and synthetic operations simultaneously occur during the process, the material properties and process variables such as temperature, pressure, gas composition, initial powder size, purity of the initial powder, pressed sample size and, thermal enthalpy can affect the process of nitriding. For this reason, the comprehensive mechanism could be very complicated, multifaceted and non-linear. All abovementioned variables make laboratory studies process very costly and time-consuming. However, overall ignoring of any singular factors in the process makes a failure in a direct comparison between the various test results.

In order to review the details on the kinetics and nature of complex reactions such as silicon nitride by reaction bonding method, modeling of the process is inevitably required. Modeling allows us to prevent trial and error as we get an acceptable beneficial trend of production both on time and cost. Previously developed models have been presented for this process are based on the diffusion mechanism of nitrogen into silicon and other mechanisms in different stages of the reaction are not comprehensively considered. The Jander model is actually a very simplified model that describe the kinetics of solid-gas reactions in general. This model has made many assumptions to be simplified, with many errors entering the results [10]. Another model is the model presented by Lee et al. that is specifically designed for silicon nitride and tries to fully consider the different mechanisms governing the process in the model [11]. This model focuses on temperature factor and other affecting parameters while the reaction kinetics is not included in this model. The model developed by Chang et al. is expressed for silicon nitride based on the mechanism of nitrogen diffusion in solid silicon nitride, however additional mechanisms governing different stages of reaction are not considered [12]. In fact, a more comprehensive mathematical model which fully describes the effect of various kinetics parameters in the reaction bonding process has been bringing into being. The model that tries to develop in this scheme is more complete than previously proposed models expressed in the kinetics of silicon nitride. In this model, the effect of numerous process factors such as process temperature, alteration in the size of the initial silicon particles, purity, particle density, and also the reactant gas pressure are examined. The impact of these factors along with the various mechanisms that govern the reactivity structure will be determined which in other presented accurate models are not systematically considered. In the present study, a comprehensive kinetics model that divides the reaction into different stages and incorporates effective kinetics parameters for the nitridation reaction of the silica powder sample in the atmosphere of nitrogen gas is developed. The suggested model interprets the percentage of reaction progression considering kinetics parameters and then tries to adapt well to the real values. Finally, the model is evaluated by performing tests and results of the model are compared with the real values attained from new data to ensure the accuracy of the model's performance.

2. RESEARCH METHOD

2.1. Analytical Modeling

Reaction bonded silicon nitride is an intrinsically complex chemical process as the kinetics of the RBSN process can be divided into three main regions. During early stages (10 to 15% of the reaction's progress), silicon nitride nucleates at the free surface of silicon that can be influenced by inherent factors such as the surface area of the powder. This nucleus can be selected as an embryo to start the next nucleation and begin the main nitridation stage. The second stage, which includes reaction progression from 10% to 70% ± 10%, forms a major part of the nitridation reaction that leads to pore filling and increasing density. Temperature and sample surface areas are supervisory factors of process rate at this stage. At the commencement of the second stage of nitridation reaction, nitrogen can easily diffuse into the structure of micropores. Though, with the gradual progression of the reaction and pore filling, nitrogen diffusion capacity is considerably reduced.

In the third step, at the final stage of nitriding, the rate of reaction progression against time is greatly reduced. In this case, the watermelon skin

[DOI: 10.22068/ijmse.16.3.52]

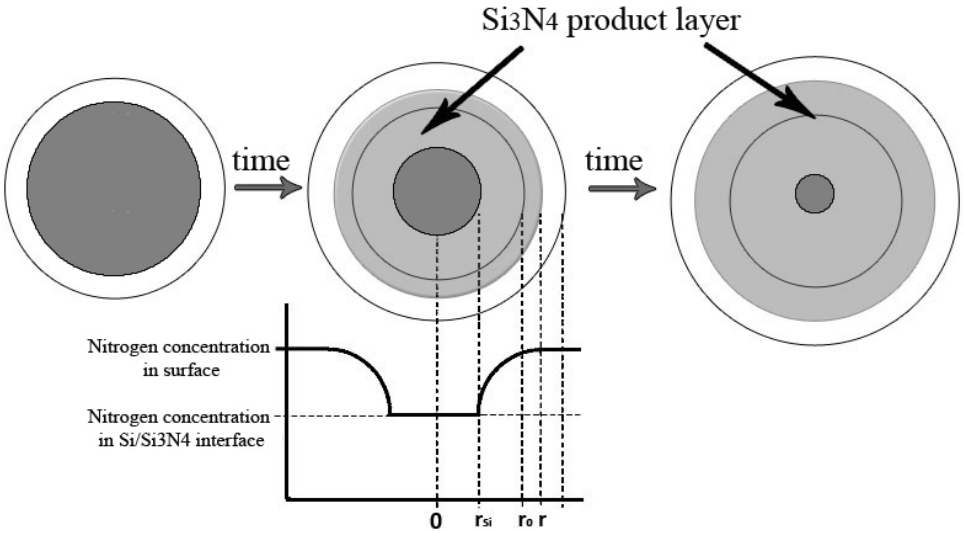

Fig.1. Schematic of the progression of nitridation reaction under a sharp interface model (nitrogen diffusion control in the product layer) r_0: initial radius of the silicon particle r: radius of the particle at time of t r_{si}: radius of unreacted silicon.

structure covers the sample surrounding that results in the non-complete reaction in large sample sizes. Under such conditions, increasing nitrogen pressure and temperature can help to increase the percentage of reaction.

2.2. Kinetic Analysis SIM

Based on the nitridation behavior of silicon and its dependency on temperature and surface area, it is suggested to use a sharp interface model for the conversion of single-particle silicon to silicon nitride. This model can well express the nitridation reaction, which includes increasing the volume of the product layer under diffusion control conditions. In fact, silicon particles are not porous therefore, the reaction occurs at the interface of silicon-silicon nitride. Fig. 1 shows a schematic illustration of the sharp interface model.

The formation of the product layer of Si_3N_4 creates a distinct interface with non-porous silicon.

In the SIM model, the rate of three processes is important:

1. Gas diffusion in the gas layer around the particle (external mass transfer)
2. Nitrogen diffusion into Si_3N_4 product layer
3. The chemical reaction at the Si-Si_3N_4 surface

2.3. Solid-gas Kinetics For Particles With a Constant Size in The Reaction

It was initially assumed that the final size of the particle in the reaction remains unchanged. r_0 (initial radius of the particle) is constant and equal to $\frac{F_p V_p}{A_p}$. So that the particle shape factor F_p, which is considered for spherical particle 3, V_p is the volume of the particle and A_p is the particle-reactive surface. Equation 1 shows the progress of the reaction by changing the time for a constant-sized particle during the reaction. The calculation method is shown in Appendix (A).

$$(9D_e C_N^0 / \rho_{si})\left(\frac{A_p}{F_p V_p}\right)^2 t = 1-3(1-X)^{\frac{2}{3}}+2(1-X) \qquad (1)$$

2.4. Kinetics of Solid-gas reaction for particles with variable size during the reaction

When the external dimensions of the particles change during the reaction, the final size is not constant and to apply this condition in the equations, parameter Z is defined as the volume change of the reaction zone. In fact, the Z parameter represents the ratio of Si_3N_4 volume which formed during nitridation to the reacted silicon volume. The final equation of reaction progression for particles with variable size during the reaction is expressed in

[DOI: 10.22068/ijmse.16.3.52]

equation (2). The calculations for determining this equation are presented in Appendix (B).

$$(\frac{3}{2}D_eC_N^0/\rho_{si}P^2)t=t^+=\frac{1}{2}\left[\frac{Z-\left[Z+(1-Z)(1-X)\right]^{2/3}}{Z-1}-(1-X)^{2/3}\right] \quad (2)$$

Equation 3 represents the linear relationship between function which is dependent upon the reaction progression (X) and time (t). In fact, by using this relationship, it is possible to control the reaction rate in different time steps for the nitridation of a silicon particle. In spherical particles, the curve is Z-dependent. In Fig. 2, the reaction progress is expressed for various Z values:

$$\frac{t^+}{t^+_{X=1}}=\frac{\frac{1}{2}\left[\frac{Z-\left[Z+(1-Z)(1-X)\right]^{\frac{2}{3}}}{Z-1}-(1-X)^{2/3}\right]}{\frac{1}{2}.\frac{\left(Z-Z^{2/3}\right)}{Z-1}} \quad (3)$$

The Jander equation for the spherical state is as follows:

$$\frac{t^+}{t^+_{X=1}}=3\left[1-(1-X)^{\frac{1}{3}}\right]^2 \quad (4)$$

Fig. 3 shows the comparison of the solutions obtained from the optimized equation (the exact solution of equation 3) with the Jander equation (Eq. 4). At the beginning of the reaction, when less nitridation is carried out, the assumptions that were considered by the Jander equation are accurate for the thinner layer of products, but these assumptions cannot be true anymore by increasing the thickness. In the meanwhile, the Jander equation does not correctly calculate the correct finishing time for the reaction.

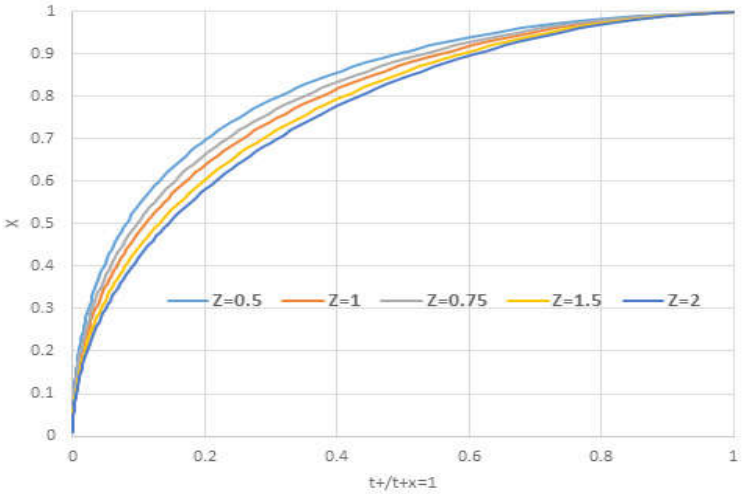

Fig. 2. Progression of the reaction for different values of Z during the process.

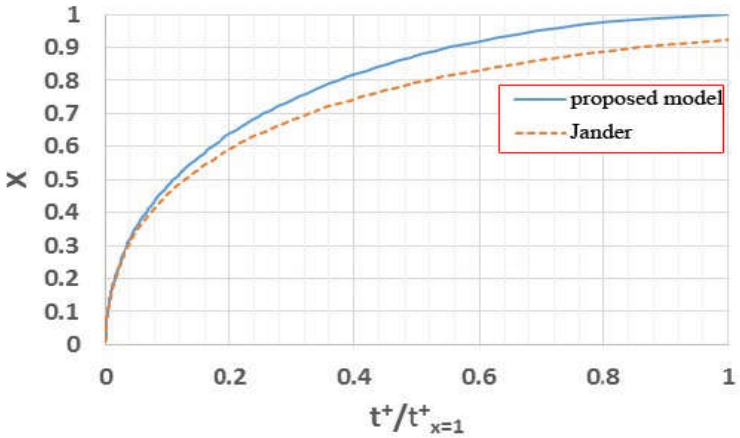

Fig. 3. Comparison of the optimal equation and the Jander equation

[DOI: 10.22068/ijmse.16.3.52]

2.5. Data Validation Experiments

For the reaction of silicon nitride, the Dongfang Resource (China) Si powder, purity 99.995 was used. Particle size analysis (PSA) was used to determine the particle size of the used silicon and the results are presented in Table 1. To prepare the samples, the powders are poured into the metal mold and pressed, initial silicon compacts were accommodated in the furnace. The weight of each specimen was measured and recorded with a laboratory balance with the accuracy of 0.001 g. Before pressing, the adhesive polyvinyl acetate (PVA) was added to samples for strength, for this purpose, 5 g of glue was added to 100 ccs of water on a hot plate then allow the mixture to be homogeneous for 24 hours after that the press operation was performed using a pressing machine under the applied pressure of 3 MPa.

2.5.1 Nitridation Process

With regard to the predictions obtained from the analytical model, there was a perspective on the time and rate of reaction. According to analytical model data at 4 different temperatures and 4 time periods, reaction progress was measured. In each series, a powder sample and pressed compacts were placed in the furnace. According to the temperature of nitridation reaction by reaction bonding method in the range 1250-1400 °C in the other works [15,16], the weight change of the samples was measured at 1275, 1300, 1325 and 1350 °C, respectively, at 4 different times. To perform the nitride reduction process, a tubular furnace with nitrogen-reactive gas (99.99% purity) together with hydrogen was used. The mixture of reactive gases was carried out (95% N_2 - 5% H_2). It should be noted that hydrogen was used to reduce the partial oxygen content of the mixture of silicon powder. Fig. 4 indicates the image of the samples after the nitridation operation.

2.5.2. Determination of Nitriding Extent

As can be inferred, the increase in compound weight is due to the addition of nitrogen to silicon and hence, by dividing the weight variation to nitrogen molecular mass, the amount of reacted silicon can be calculated by using stoichiometric relationships. Equation 5 indicates the progression of the reaction. In this equation, is the percentage of reaction progression, ,weight change equal to the amount of nitrogen added to the stoichiometry during the nitridation reaction, is the initial weight of the sample, is the molecular mass of the silicon and is the molecular mass of nitrogen. The calculation method is in Appendix (C).

Table 1. Specifications of the powder used in the experiment

Particle size (µm)	Special surface) ($\frac{m}{g}$)	Particle size distribution (µm)			σ (Standard Deviation)
		D10	D50	D90	
4.76	1.69 ± 0.02	1.26	4.76	13.66	2.18

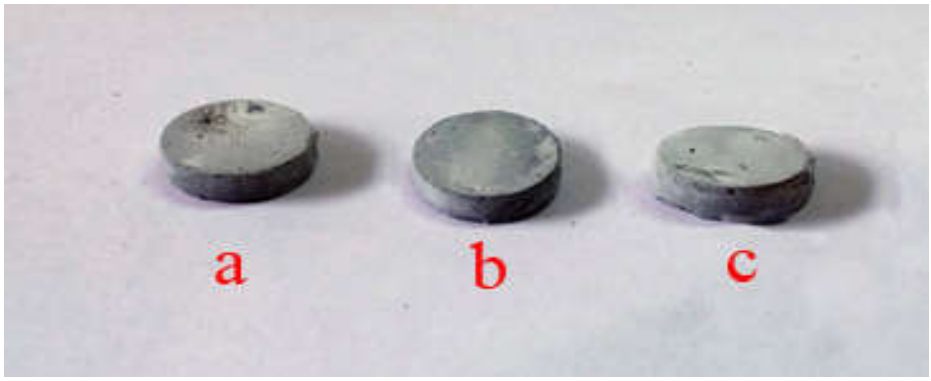

Fig. 4. Illustration of samples after nitriding in different temperature a) 1275 C b) 1300 C c) 1325 C

[DOI: 10.22068/ijmse.16.3.52]

Table 2. Weight variations at different temperatures

Temperature (°C)	Sample weight after reaction (g)	Initial weight (g)	Weight Change	X	Time (h)
1275	0.478	0.438	0.04	0.138	0.5
1275	0.413	0.304	0.109	0.541	1
1275	0.495	0.307	0.188	0.917	5
1275	0.342	0.208	0.134	0.968	8
1300	0.429	0.325	0.104	0.483	0.5
1300	0.52	0.371	0.149	0.604	1
1300	0.486	0.304	0.182	0.895	3
1300	0.496	0.299	0.197	0.991	5h 18min
1325	0.374	0.271	0.103	0.573	0.5
1325	0.506	0.339	0.167	0.742	1
1325	0.615	0.382	0.233	0.918	2
1325	0.252	0.152	0.1	0.985	4
1350	0.194	0.134	0.06	0.679	0.5
1350	0.413	0.266	0.147	0.827	1
1350	0.495	0.310	0.185	0.894	1.5
1350	0.523	0.317	0.206	0.977	2.5

$$X = \frac{3M_{Si}\Delta W}{2M_{N_2}W_0} \quad (5)$$

According to the above mathematical description, the reaction progression was calculated in different temperature and time conditions by using sample weight change being reported in Table 2.

3. RESULTS AND DISCUSSION

In Fig. 5, the reaction progress rate was calculated by equation (2). In this regard, effective diffusion has been extracted from references [11,13] and the parameter Z of sample expansion calculated 1.26 which is explained in Appendix (d).

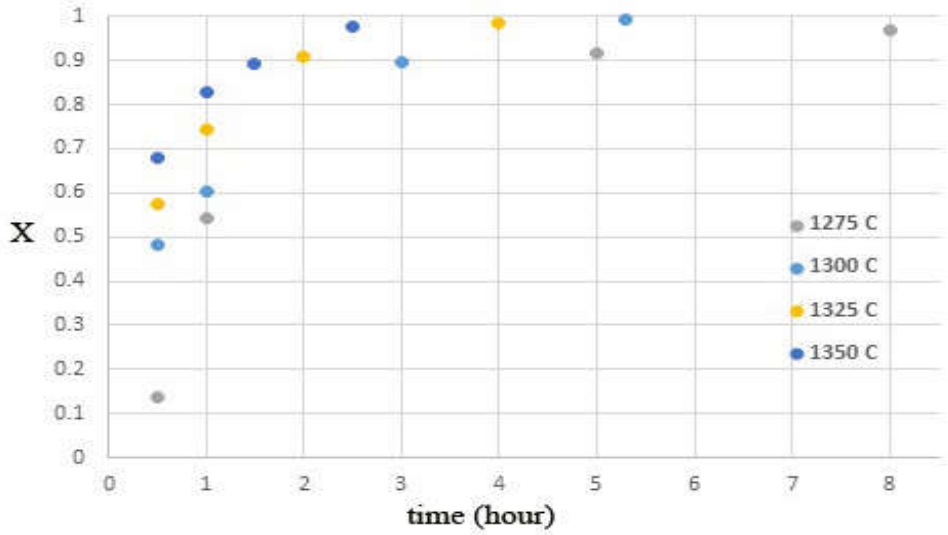

Fig. 5. Reaction progresses at different times for temperatures of 1275, 1300, 1325 and 1350 °C

[DOI: 10.22068/ijmse.16.3.52]

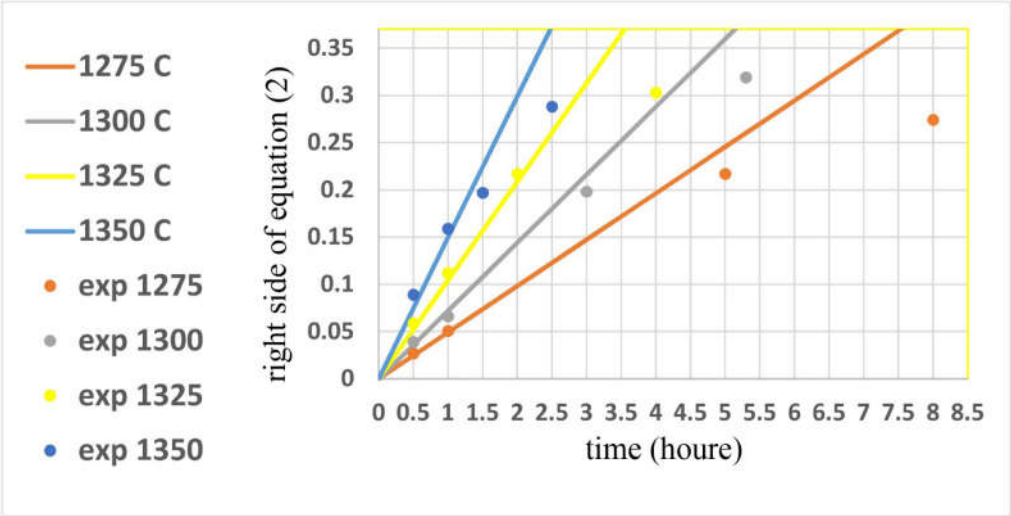

Fig. 6. Comparison of data obtained from experimental results and calculated values from the analytical model

The ideal gas law was used to calculate nitrogen gas concentrations while the particle radius calculated in the particle size distribution experimental route. The calculated values for the concentration is $41*10^{-6} mol/Cm^3$, and the calculation method is shown in Appendix (E).

To obtain the value of the right side of equation 2, the experimental value of X and Z at the right side of the equation should be known. The results are compared in Fig. 6.

3.1. Statistical Error Parameters

In order to analyze the performance of the developed model, the statistical error parameters have been used: mean absolute error (MAE), root mean square error (RMSE), correlation coefficient (R) and coefficient of determination (R^2). Fig. 7 shows the statistical calculation of the error for the data.

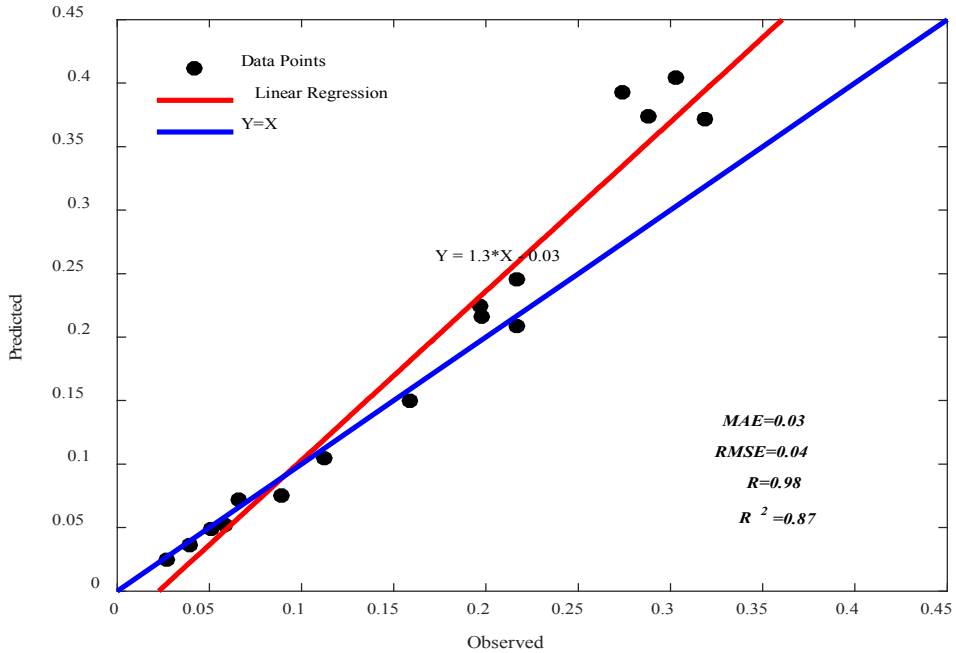

Fig. 7. ross validation graph and calculated error values

[DOI: 10.22068/ijmse.16.3.52]

$$MAE = \frac{\sum_{i=1}^{N} |P_i - O_i|}{N} \quad (6)$$

$$RMSE = \sqrt{\frac{1}{N}\sum_{i=1}^{N}(P_i - O_i)^2} \quad (7)$$

$$R = \frac{\sum_{i=1}^{N}(P_i - P_m)(O_i - O_m)}{\sqrt{(P_i - P_m)^2}\sqrt{(O_i - O_m)^2}} \quad (8)$$

$$R^2 = 1 - \frac{\sum_{i=1}^{N}(O_i - P_i)^2}{\sum_{i=1}^{N}(O_i - O_m)^2} \quad (9)$$

Where O_i is the measured value, P_i is the predicted value, N is the number of data, O_m is the mean of the measured values and P_m is the average of the predicted values.

Fig. 8 actually shows the duration time that takes to complete the reaction with 100% conversion. In this figure, the obtained values of the analytical model and the experimental results are compared and the results are in good agreement. To obtain the completion time of the reaction, simply the value of X in equation 2 should be put equal to 1. In this case, the right side of the equation is equal to the constant value of 0.355. The diffusion coefficient is also replaced by the exponential function of temperature in equation 2. Equation 10 is the final outcome of relation 2, which calculates the time required for the completion of the nitridation at various temperatures. By plotting the time-temperature diagram, the completion time of reaction for each temperature can be consequently obtained.

$$\frac{(3*14.27\exp(\frac{-310kj}{8.314T})*0.000041*28*3600)t}{(2.33*0.00000238^2)} = 0.355 \quad (10)$$

As mentioned, the effective diffusion coefficient using experimental data can be computed by the terms proposed in equation 2. The value of X and time for 4 points of 4 different temperatures are determined in the experiment and are presented in Table 2. By using these data and equation 2, we can obtain the effective diffusion coefficient and compare them with the values that were deliberately extracted from the references. Fig. 9 shows a comparison between the effective diffusion coefficient used in the analytical model and the diffusion coefficient obtained from the experimental data. According to the results of the comparison shown in fig. 9, there is an acceptable agreement between experimental data and other references [11,13]: (The dash line curve of Fig. 9 represents the relation of 11)

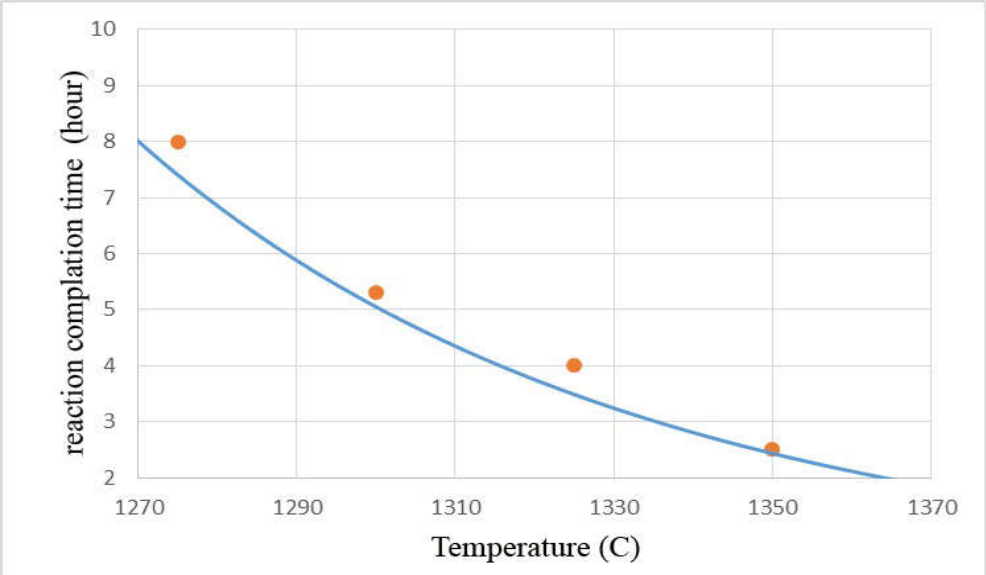

Fig. 8. Comparison of the completion time of the reaction obtained from the model and the experimental results

[DOI: 10.22068/ijmse.16.3.52]

$$(\frac{3}{2}D_eC_N^0 / \rho_s P^2)t = t^+ = \frac{1}{2}\left[\frac{Z-\left[Z+(1-Z)(1-X)\right]^{\frac{2}{3}}}{Z-1}-(1-X)^{2/3}\right]$$

$$\frac{3*D_{eff}*0.000041\left(\frac{mol}{cm^3}\right)*28\left(\frac{g}{mol}\right)*3600\left(\frac{s}{h}\right))*time(h)}{2.33\left(\frac{g}{cm^3}\right)*(0.00000238(cm))^2} = Right\ side\ of\ \ Equation\ (2)$$

$$D_{eff} = 14.275\exp\left(-\frac{310(kj)}{RT}\right)$$

$$LnD_{eff} = Ln(14.275)+\left(-\frac{310(kj)}{RT}\right) \quad (11)$$

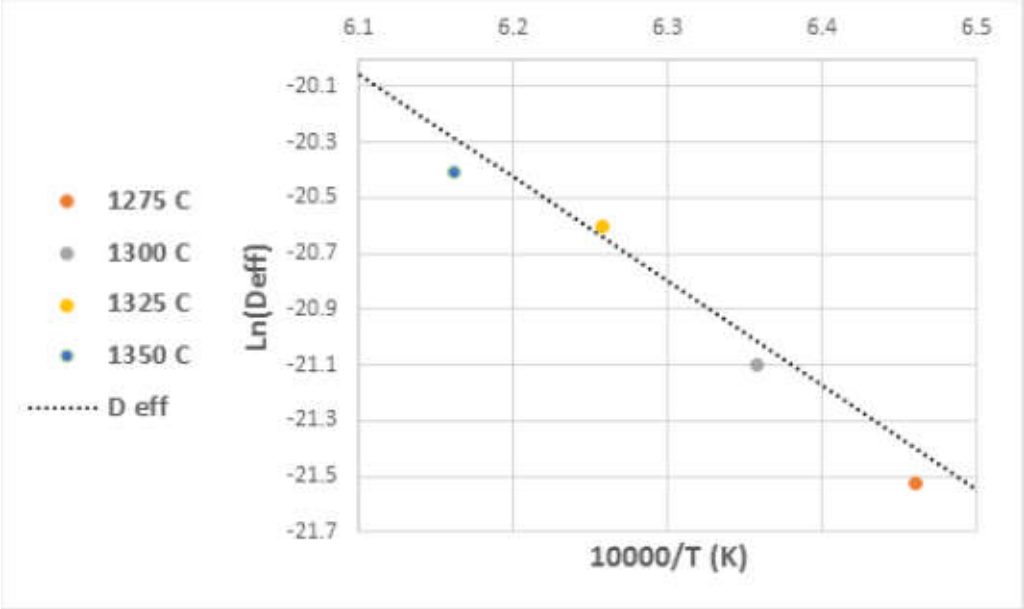

Fig. 9. Comparison of the effective diffusion coefficient used in the model (dash line) and the results of experimental data (colored points)

The good superposition between experimental data and the analytical results from model indicates the proper functioning of the SIM model for this reaction. The hypothesis of the diffusion control condition in the linear region or second stage of the reaction kinetics predicts the kinetic behavior of the reaction well. Though, in the final stages of the reaction due to the complexity of the involved diffusion mechanism, including network diffusion, the model deviates from the experimental values. In general, the results are very impressive compared to the previous models and introduce a relatively more efficient and accurate kinetics model of reaction with diffusion control conditions. The microstructure of the nitrided sample at 1350 °C was studied after initial preparation using a scanning electron microscope (SEM) (Fig. 10)

[DOI: 10.22068/ijmse.16.3.52]

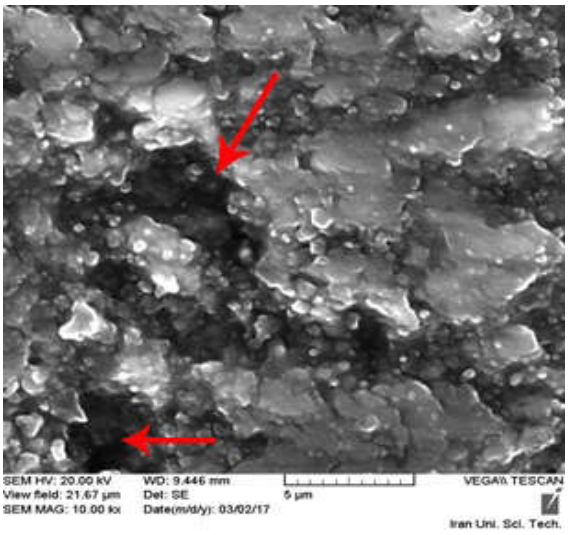

Fig. 10. SEM microstructure of nitride sample treated at 1350 °C. voids shown by arrows

To inspect the interior of the compound, one of the compact sample was cut into two halves using a cutting machine and the cutting surface was studied. Fig. 11 shows the EDS analysis of the nitrided sample in cross-section which clearly displays the distribution of nitrogen in the sample. The red dots indicate the distribution of nitrogen and orange ones indicate the distribution of silicon. Black zones, free of nitrogen and silicon, are porous areas of the sample.

In XRD analysis, three samples at 1325 °C were investigated at three-time points with reaction progression of 54%, 72% and 91% that in all of them, conversion of silicon to silicon nitride has taken up to a high percentage.

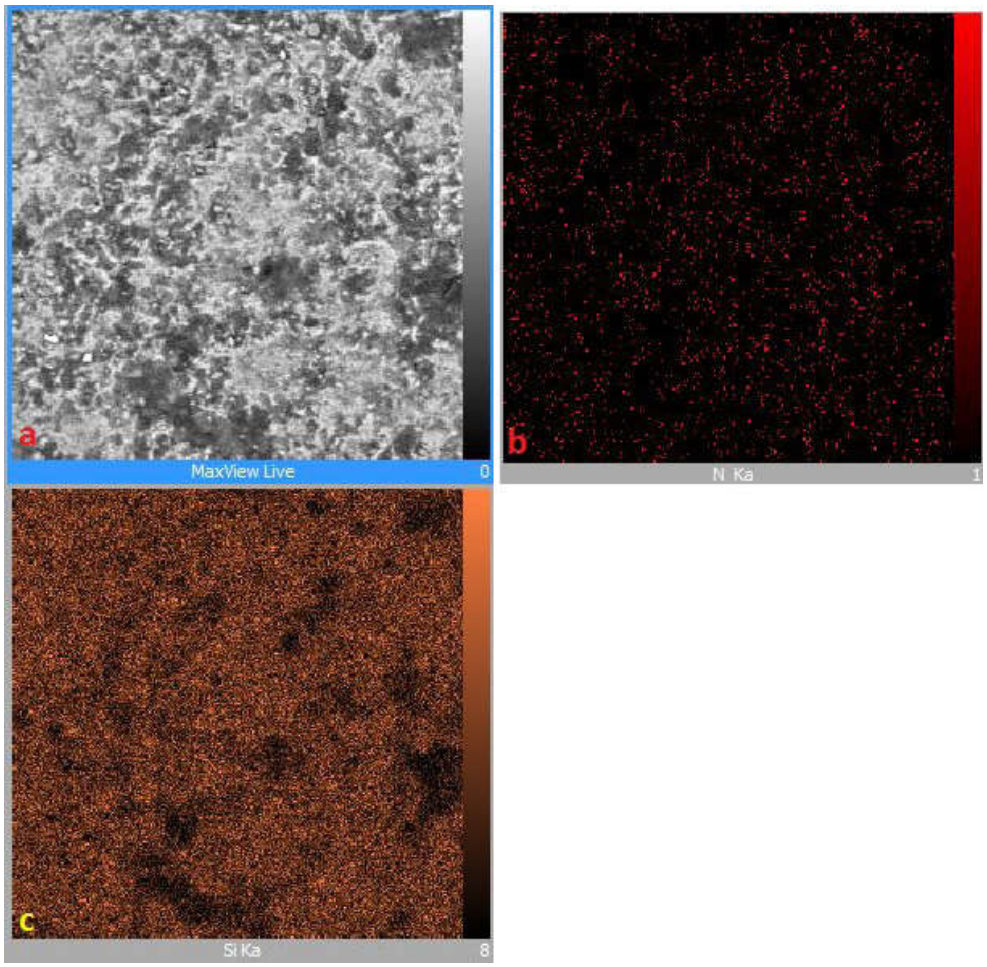

Fig. 11. EDS analysis from the surface of nitride sample
a) Cross-section microstructure b) Nitrogen distribution c) Silicon distribution

[DOI: 10.22068/ijmse.16.3.52]

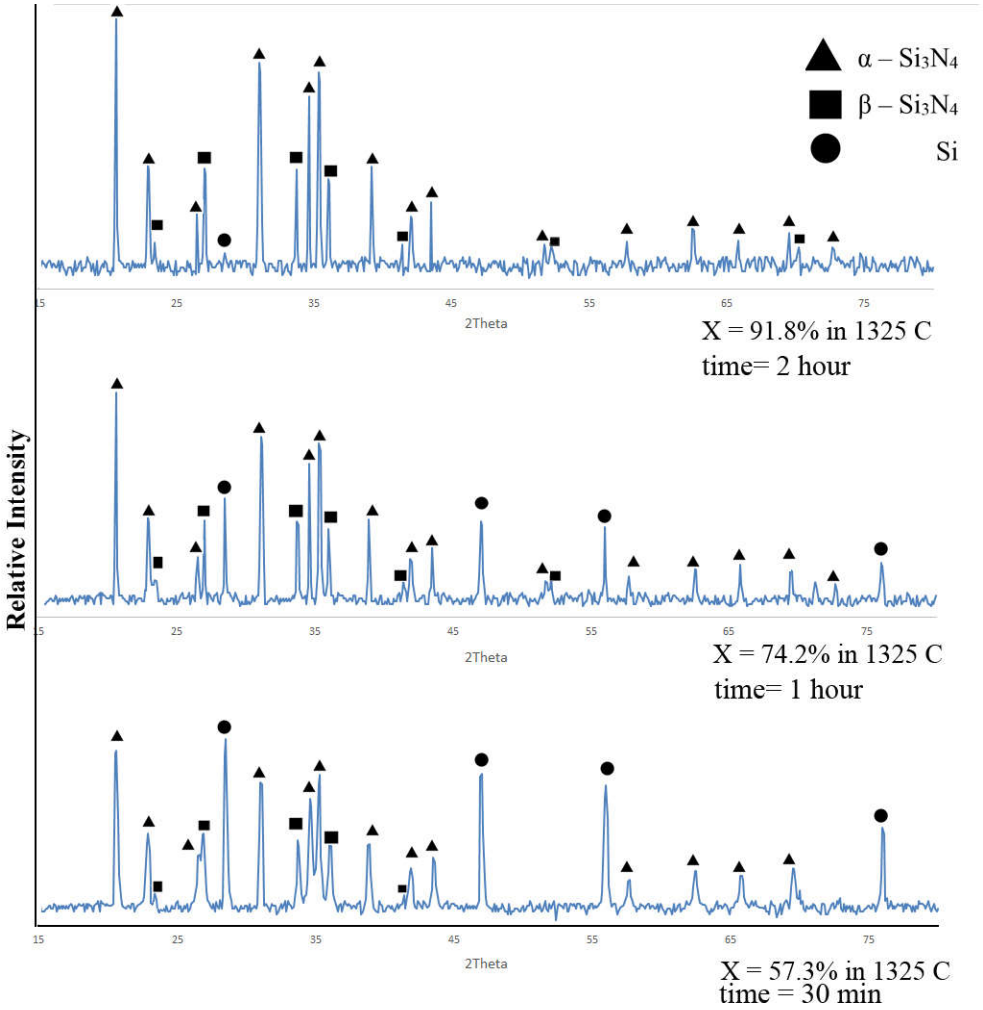

Fig. 12. Phases formed by the progression of nitride reaction at 1325°C for 30 minutes, 1 hour and 2 hours

The analysis proves the fact that the reactant gas is well diffused in the sample and the nitridation has occurred within the sample. A point analysis of the sample surface clearly demonstrates the presence of the element Si, N in the final sample and due to the absence of other gases in the vacuum environment with the ideal thermodynamic condition for the formation of silicon nitride, there is no effective impurity in the reaction products.

4. CONCLUSION

In this investigation, an attempt was made to produce Si_3N_4 via reaction bonded method. In addition, an analytical model was proposed to predict the kinetics of silicon nitridation process by such a method. The following results can be highlighted:

1. Excellent correlation between experimental data and model's response that suggest the mechanism of SIM to be based on diffusion control as the dominant mechanism of reaction in most reaction time.
2. Considering the dominant mechanism in the reaction's progress, the analytical model can provide acceptable predictions although the process is quite complex.
3. By applying the SIM model to the reaction of silicon nitride reaction bonding, the first attempt for the development of such model was done.

[DOI: 10.22068/ijmse.16.3.52]

4. The proposed model has high flexibility when compared to previous models that considered fewer variables and reaction conditions with higher performance. The suggested model predictions were more accurate and are able to apply to other chemical reactions that have similar kinetic conditions.

REFERENCE

1. Golla, B. R., Ko, J. M. Kim, J. W., and Kim, H.D., "Effect of particle size and oxygen content of Si on processing, microstructure and thermal conductivity of sintered reaction bonded Si_3N_4", J. Alloy.Compd., 2014, 595, 60–66.
2. Chen, F, Shen,Q., Yan, F., and Zhang, L., "Pressureless Sintering of Si_3N_4 Porous Ceramics Using a H_3PO_4 Pore-Forming Agent", J. Am.Ceram.Soc., 2007, 90, 2379-2383.
3. Cheng, H., Li, Y., Kroke, E., Herkenhoff, S., "In situ synthesis of Si_2N_2O/Si_3N_4 composite ceramics using polysilyloxycarbodiimide precursors", J. Eur.Ceram.Soc. 2013, 33, 2181-2189.
4. Wu, Z., Zhang, Z., Yun, J., Yan, J., and You, T., "Synthesis of α-Si_3N_4 crystallon by a solvothermal method at a low temperature of 180°C", Physica. B. Condens. Matter., 2013, 428, 10-13.
5. Kita, H., Hirao, K., Hyuga, H., Hotta, M., and Kondo, N., "Review and Overview of Silicon Nitride and SiAlON, Including their Applications", Handbook of Advanced Ceramics, Elsevier, 2013, 245–266.
6. Wasanapiarnpong,T., Wada, S., Imai, M., and Yano, T., "Effect of post-sintering heat-treatment on thermal and mechanical properties of Si_3N_4 ceramics sintered with different additives", J. Eur.Ceram.Soc. 2006, 26, 3467-3475
7. Hirao, K., Zhou, Y., Hyuga, H., Ohji, T., and Kusano, D., "High Thermal Conductivity Silicon Nitride Ceramics", J. Korean.Ceram. Soc., 2012, 49, 380-384
8. Gilissen, R., Erauw, J. P., Smolders, A., "Vanswijgenhoven, E., and Luyten, J., Gelcasting, a near net shape techniquent", Mater Des., 2000, 21, 251-257.
9. Cano, I. G., Pérez Baelo, S., Rodríguez, M. A., de Aza, S., "Self-propagating high temperature-synthesis of Si_3N_4: role of ammonium salt addition", J. Eur.Ceram.Soc. 2001, 21, 291-295.
10. Kingery, U.D., Bowen, HK, Introduction to Ceramics, Wiley, New York, 1976, 234-246.
11. Li, W.B., Lei, B.Q., Lindbäck, T., A kinetic model for the reaction bonding process of silicon powder compact, J.Eur.Ceram.Soc. 1997, 17, 1119-1131
12. Chang, F. W., Liou, T. H., Tsai, F. M., "The nitridation kinetics of silicon powder compacts", Thermochim. Acta. 2000, 354, 71-80.
13. Jennings, H. M., "On reactions between silicon and nitrogen", J. Mater. Sci. 1983, 18, 951-967
14. Park, C. P. D., Kim, H., Lim, K. T., Bang, K., "Microstructure of reaction-bonded silicon nitride fabricated under static nitrogen pressure", Mater. Sci. Eng. A., 2005, 405, 158–162.
15. Jennings, Hamlin M., Richman, Marc, H., "Structure, formation mechanisms and kinetics of reaction-bonded silicon nitride", J. Mater. Sci. 1976, 11, 2087–2098.
16. Chang, F. T. F., Liou, T., "The nitridation kinetics of silicon powder compacts", Thermochim. Acta. 2000, 354, 71–80.

[DOI: 10.22068/ijmse.16.3.52]

Appendix (A) - Calculations of reaction kinetics for a particle with constant size in gas-solid reactions

r_c or radius of the reaction surface changes with time as the reaction progresses within the particle. Considering these cases, we declare the reaction rate according to Fig. 13 as following:

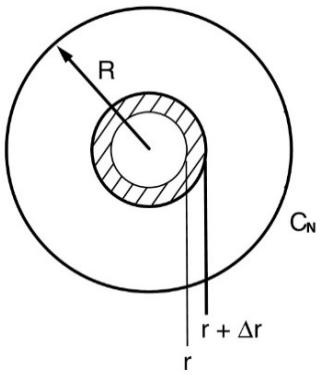

Fig. 13. Nitrogen diffusion in a spherical particle

$$\text{Reaction rate} = -4\pi r_c^2 \rho_s \frac{dr_c}{dt} \qquad (12)$$

According to the SIM model, the total rate of diffusion and reaction rate is equalized and we derive integral from the resulting equation:

$$4\pi r_c^2 \rho_s \frac{dr_c}{dt} = \frac{3}{2}.4\pi D_e C_N^0 / \left(\frac{1}{r_c} - \frac{1}{r_0}\right) \qquad (13)$$

$$\int \left(\frac{r_c^2}{r_0} - r_c\right) dr_c = \int \frac{3}{2} D_e C_N^0 / \rho_s dt$$

$$\frac{r_c^3}{3r_0} - \frac{r_c^2}{2} + A = (\frac{3}{2} D_e C_N^0 / \rho_s) t$$

The boundary conditions are:

$$@t = 0 \quad r_c = \frac{F_p V_p}{A_p}$$

$$@r = r_c \quad C_N = 0$$

On the other hand, the initial reaction level is equal to the initial radius of the particle $r_0 = \frac{F_p V_p}{A_p}$. With progressing of the reaction, the radius of the reaction front is shown by $r_c = \eta_c \frac{F_p V_p}{A_p}$ and η_c is the dimensionless position of the reaction front, which its relationship with the reaction percentage expressed as follows:

$$X = 1 - \eta_c^{F_p}$$

For ease of calculation, the shape factor of particle shape considered P:

$$P = \frac{F_p V_p}{A_p}$$

Now we apply the boundary condition for obtaining the integral constant A:

$$A = \frac{P^2}{6}$$

Now, in equation 13, we replace the values of A, r_c, and r_0:

$$\frac{(\eta_c P)^3}{3P} - \frac{(\eta_c P)^2}{2} + \frac{P^2}{6} = \left(\frac{3}{2} D_e C_N^0 / \rho_s\right) t$$

$$(9 D_e C_N^0 / \rho_s) \left(\frac{A_p}{F_p V_p}\right)^2 t = 1 - 3\eta_c^2 + 2\eta_c^3$$

$$X = 1 - \eta_c^{F_p}$$

By replacing the reaction percentage with the dimensionless position of the reaction front, the above equation will be as follows:

$$(9 D_e C_N^0 / \rho_s) \left(\frac{A_p}{F_p V_p}\right)^2 t = 1 - 3(1-X)^{\frac{2}{3}} + 2(1-X) \qquad (1)$$

[DOI: 10.22068/ijmse.16.3.52]

Appendix (B)- Kinetic calculations of the nitridation reaction for a variable-size particle in solid-gas Reactions

In the calculations, the Z parameter is expressed as equation 14. In this regard, r is the current size of the particle, r_0 is the initial size of the particle and r_c is the reaction front radius.

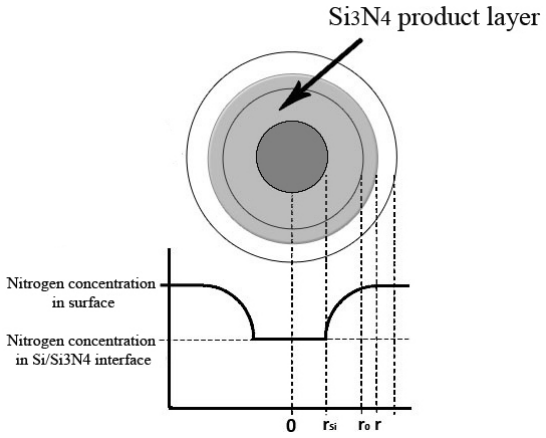

Fig. 14. The expression of the radial parameters used in relation 14

$$Z = \frac{r^3 - r_c^3}{r_0^3 - r_c^3} \qquad (14)$$

$$r = \left(\frac{F_p V_p}{A_p}\right)_t$$

$$r_0 = \left(\frac{F_p V_p}{A_p}\right)_{initail}$$

$$r_c = \eta_c \left(\frac{F_p V_p}{A_p}\right)_{initial}$$

$$\eta_c^3 = (1-X)$$

According to the above equations:

$$\left(\frac{F_p V_p}{A_p}\right)^3_t = Z\left(\frac{F_p V_p}{A_p}\right)^3_{initial} + (1-Z) r_c^3$$

$$\left(\frac{F_p V_p}{A_p}\right)_t = Z\left(\frac{F_p V_p}{A_p}\right)^3_{initial} + (1-Z) h_c \left(\frac{F_p V_p}{A_p}\right)^3_{initial}$$

$$p = \left(\frac{F_p V_p}{A_p}\right)$$

$$r_0 = \left[Z + (1-Z)(1-X)\right]^{1/3} . p$$

$$r_c = (1-X)^{1/3} P \qquad dr_c = \frac{-P}{3(1-X)^{2/3}} dX$$

$$\int \left(\frac{r_c^2}{r_0} - r_c\right) dr_c = \int \left[\frac{(1-X)^{\frac{2}{3}} P^2 \left(\frac{-1}{(1-X)^{\frac{2}{3}}}\right)}{\left[Z + (1-Z)(1-X)\right]^{\frac{1}{3}}} - (1-X)^{1/3} P \frac{-1}{3(1-X)^{2/3}}\right]$$

$$\int P^2 \left[\frac{-1}{3\left[Z + (1-Z)(1-X)\right]^{\frac{1}{3}}} + \frac{-1}{3(1-X)^{1/3}}\right] dX$$

$$= P^2 \left[\frac{-\left[Z + (1-Z)(1-X)\right]^{\frac{2}{3}}}{2(Z-1)} - \frac{(1-X)^{\frac{2}{3}}}{2}\right] + Const$$

B.C.:

$$@t = 0 \;\; X = 0 \rightarrow Const = P^2[1/2(Z+1) + 1/2] = P^2[Z/(2(Z-1))]$$

Finally, equation 2 defined reaction progression for a spherical particle with the variable as follows. In this equation, the t^+ dimensionless time required to reaction progression of X and $t^+_{x=1}$ is dimensionless time to complete the reaction.

$$\left(\frac{3}{2} D_e C_N^0 / \rho_s P^2\right) t = t^+ = \frac{1}{2}\left[\frac{Z - \left[Z + (1-Z)(1-X)\right]^{2/3}}{Z-1} - (1-X)^{2/3}\right] \qquad (2)$$

[DOI: 10.22068/ijmse.16.3.52]

Appendix (C) - Calculations of the reaction progression based on weight change of nitride samples

$$3Si + 2N_2 = Si_3N_4$$

$$\Delta W = \text{Weight of } N_4 \text{ in } Si_3N_4 (g)$$

$$\frac{\Delta W}{2M_{N_2}} = mol_N = mol_{Si\,3N\,4}$$

$$\frac{\Delta W}{2M_{N_2}} = mol_N = mol_{Si\,3N\,4}$$

$$\left(\frac{\Delta W}{2M_{N_2}}.3\right).M_{Si} = gr_{Si}$$

$$X = \frac{3M_{Si}\Delta W}{2M_{N_2}W_0}$$

Appendix (D) - Calculation of parameter z for the nitridation of silicon

$$Z = (\frac{M_w}{\rho})_{Si\,3N\,4}(\frac{\rho}{M_w})_{Si}\left(\frac{\text{Si3N4 Stoichiometric coefficient}}{\text{Si Stoichiometric coefficient}}\right)$$

( ) ( ) 3 1.216

$$Z = (\frac{140\,g}{\frac{3.19g}{cm\,3}})_{Si\,3N\,4}(\frac{\frac{2.33g}{cm\,3}}{M_w})_{Si}\left(\frac{1}{3}\right) = 1.216$$

Appendix (E) - Nitrogen concentration calculation in the reaction environment

$$PV = nRT$$

$$C = n/V$$

$$n/v = P/RT \rightarrow C = P/RT$$

$$C_N^0 = 101325Pa/(8.314*3000K) = 41*10^{-6}mol/Cm^3$$

[DOI: 10.22068/ijmse.16.3.52]